Design and Synthesis of Substrate and Intermediate Analogue Inhibitors of *S*-Ribosylhomocysteinase‡

Gang Shen,§ Rakhi Rajan,⊥ Jinge Zhu,§ Charles E. Bell,⊥ and Dehua Pei*,§

Departments of Chemistry and of Molecular and Cellular Biochemistry, Ohio State Biochemistry Program, The Ohio State University, 100 West 18th Avenue, Columbus, Ohio 43210

Received January 13, 2006

S-Ribosylhomocysteinase (LuxS) catalyzes the cleavage of the thioether linkage in *S*-ribosylhomocysteine (SRH) to produce homocysteine and 4,5-dihydroxy-2,3-pentanedione, the precursor of autoinducer 2. Inhibitors of LuxS should interfere with bacterial interspecies communication and potentially provide a novel class of antibacterial agents. LuxS utilizes a divalent metal ion as a Lewis acid during catalysis. In this work, a series of structural analogues of the substrate SRH and a 2-ketone intermediate were designed and synthesized. Kinetic studies indicate that the compounds act as reversible, competitive inhibitors against LuxS, with the most potent inhibitors having K_I values in the submicromolar range. These represent the most potent LuxS inhibitors that have been reported to date. Cocrystal structures of LuxS bound with two of the inhibitors largely confirmed the design principles, i.e., the importance of both the homocysteine and ribose moieties in high-affinity binding to the LuxS active site.

Introduction

Quorum sensing (QS[a]) is one type of bacterial cell-to-cell communication, which regulates a diverse array of physiological and pathological activities in bacteria in a cell-density-dependent manner.[1] QS is mediated by the synthesis, release, and detection of small signaling molecules, called autoinducers (AIs). There are two major types of QS systems. Type I QS is species specific, with each bacterial species having a unique AI-1 molecule or in some cases a unique combination of AI-1 molecules. Gram-negative bacteria generally use acylhomoserine lactones (AHLs) as their AI-1's, whereas Gram-positive bacteria employ oligopeptides or modified oligopeptides. Correspondingly, each species possesses a cognate AI-1 receptor protein to recognize and respond to the signal. Since the interactions between AI-1's and their cognate receptors are highly specific, AI-1's generally do not cause any cross talk in mixed populations of bacteria. To sense the presence of other species in a mixed population (interspecies communication), bacteria utilize an alternative mechanism (type II QS) in which a common signal, AI-2, is released and detected.[2,3] AI-2 has been identified as a furanosyl borate diester in *Vibrio harveyi*, by determining the X-ray crystal structure of LuxP in complex with the active AI-2 ligand.[4] Very recently, the same team showed that active AI-2 in *Salmonella typhimurium* is (2*R*,4*S*)-2-methyl-2,3,3,4-tetrahydroxytetrahydrofuran (R-THMF).[5] AI-2 is biosynthesized from *S*-adenosylhomocysteine (SAH), which is hydrolyzed by nucleosidase Pfs into adenine and *S*-ribosylhomocysteine (SRH).[6] SRH is next converted into homocysteine (Hcys) and 4,5-dihydroxy-2,3-pentanedione (DPD) by *S*-ribosylhomocysteinase (LuxS). DPD is unstable and spontaneously cyclizes to form R-THMF (*S. typhimurium* AI-2[5]) and (2*S*,4*S*)-2-methyl-2,3,3,4-tetrahydroxytetrahydrofuran, which spontaneously forms a complex with borate as *V. harveyi* AI-2.[4]

Since QS controls many bacterial behaviors including biofilm formation and bacterial virulence, proteins involved in quorum sensing are being explored as novel targets for antibacterial drug design.[7−9] Halogenated furanone derivatives have been shown to act as AI-1 antagonists and inhibit the expression of virulence factors by *Pseudomonas aeruginosa* and increase bacterial susceptibility to the antibiotic tobramycin.[10−12] In a mouse pulmonary infection model, the drug inhibited quorum sensing of the infecting bacteria and promoted their clearance by the mouse immune response.[12] Suga and co-workers synthesized a series of AHL analogues, some of which acted as antagonists of quorum sensing and interfered with virulence expression and biofilm formation by *P. aeruginosa*.[13,14] LuxS/AI-2 also regulates a host of bacterial behaviors including virulence, biofilm formation, motility, toxin and antibiotic production, luminescence, and ABC transporter expression.[7] Further, the *luxS* gene is present in the majority of Gram-positive and Gram-negative bacteria and is highly conserved.[7] Thus, AI-2 antagonists and LuxS inhibitors have the potential as a class of unconventional, broad-spectrum antibacterial agents. Two SRH analogues have recently been reported as weak inhibitors of LuxS ($IC_{50} \approx 1$ mM),[15] but potent LuxS inhibitors are still lacking. In this work, a series of substrate and intermediate analogues have been synthesized and tested for inhibition against LuxS, and the best compounds showed K_I values in the high nanomolar range.

Chemistry

LuxS is a metalloenzyme containing an Fe^{2+} ion coordinated by His-54, His-58, and Cys-126 (amino acid numbering in *Bacillus subtilis* LuxS) and a water molecule.[16−19] The native enzyme is unstable under aerobic conditions, undergoing oxidation of the Fe^{2+} ion and loss of enzymatic activity.[16] Substitution of Co^{2+} for the native metal ion produces a highly stable variant of essentially wild-type catalytic activity, whereas the Zn^{2+}-substituted enzyme has ∼10-fold lower activity.[16] In the proposed catalytic mechanism of LuxS (Figure 1), the metal ion acts as a Lewis acid, facilitating two consecutive aldose−ketose isomerization steps and a final β-elimination reaction.[20]

* To whom correspondence should be addressed. Phone: (614) 688-4068. Fax: (614) 292-1532. E-mail: pei.3@osu.edu.

‡ The coordinates of the structures of Co-BsLuxS in complex with compounds **10** and **11** have been deposited in the Protein Data Bank under accession numbers 2FQT and 2FQO, respectively.

§ Department of Chemistry.

⊥ Department of Molecular and Cellular Biochemistry.

[a] Abbreviations: AHL, acylhomoserine lactone; AI, autoinducer; DPD, 4,5-dihydroxy-2,3-pentanedione; DTNB, 5,5′-dithiobis(2-nitrobenzoic acid); Hcys, homocysteine; QS, quorum sensing; R-THMF, (2*R*,4*S*)-2-methyl-2,3,3,4-tetrahydroxytetrahydrofuran; SAH, *S*-adenosylhomocysteine; SRH, *S*-ribosylhomocysteine.

10.1021/jm060047g CCC: $33.50 © 2006 American Chemical Society
Published on Web 04/14/2006

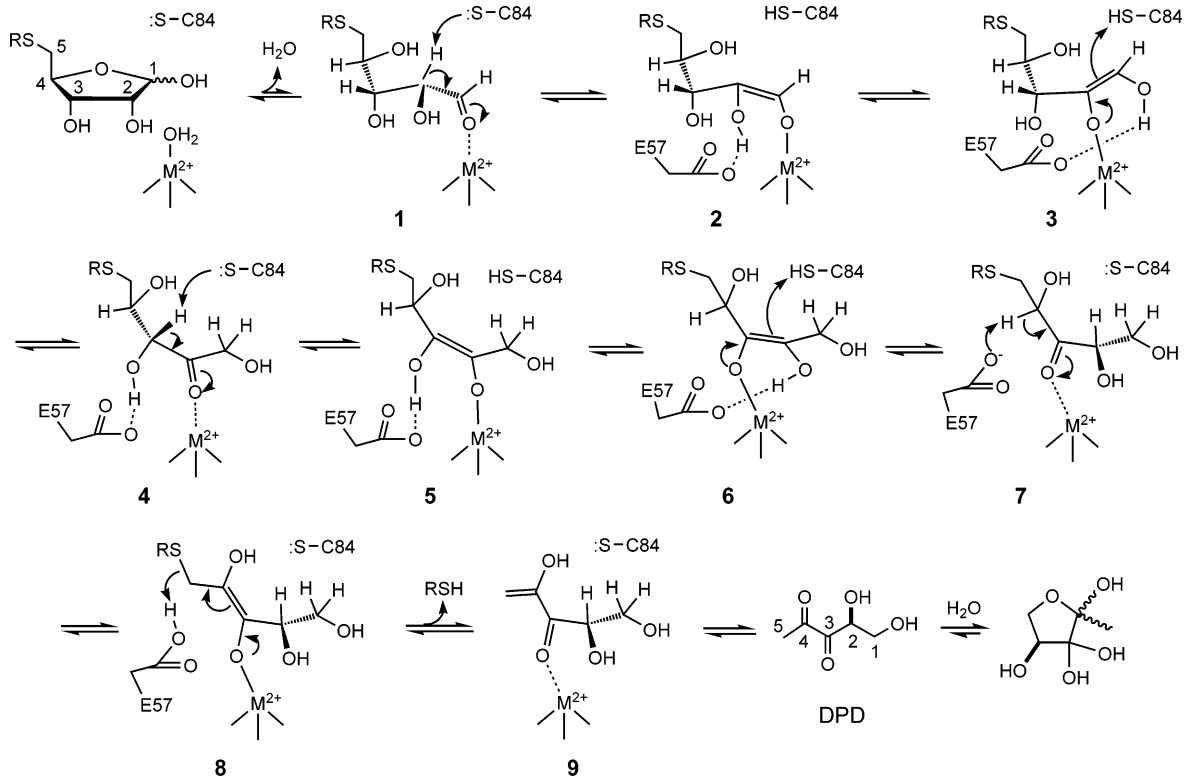

Figure 1. Proposed mechanism for LuxS-catalyzed reaction. RSH = homocysteine.

UV−vis absorption spectroscopy[16] and X-ray crystallographic studies[21] revealed that the catalytic metal ion is directly coordinated with the C-2 carbonyl oxygen of a 2-ketone intermediate (compound **4** in Figure 1). During the conversion of SRH to intermediate **4** or from intermediate **4** to 3-ketone intermediate **7**, it was proposed that the metal ion plays a key role in stabilizing the enediolate intermediates (**2**, **3**, **5**, and **6**) by binding to them in a bidentate manner (Figures 1 and 2A). We envisioned that replacement of the unstable enediolate moiety with a planar hydroxamate group (compound **10**) should produce a stable isostere with high affinity and specificity for LuxS (Figure 2). Compound **11**, which is an stereoisomer of **10** with opposite stereochemical configuration at the β carbon (relative to the hydroxamate), and compound **12**, which does not contain the Hcys moiety, were synthesized for comparison. The X-ray crystal structure of LuxS bound to intermediate **4** shows that the main interactions between the intermediate and the protein are mediated by the two termini of the compound; i.e., the amino and carboxyl groups of the Hcys moiety fit into a pocket remote from the active site, formed by residues Lys-35, Arg-65, Asp-78, Ile-79, and Ser-80, whereas the ribose is bound to the metal center.[21] There is little direct interaction between the hydrophobic linker of compound **4** and the active site. Therefore, we also designed compounds **13**−**16**, in which the amino acid moiety and a metal chelating group (thiol or *N*-formylhydroxylamine) are connected with linkers of varying lengths (Figure 2).

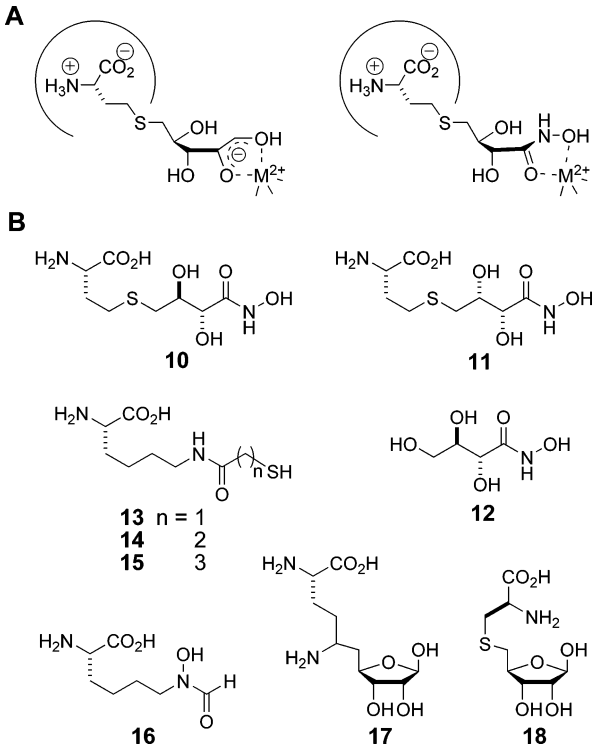

Figure 2. (A) Proposed modes of interaction among the LuxS metal center, 2-ketone intermediate **4**, and inhibitor **10**. (B) Structures of inhibitors **10**−**18**.

Synthesis of compound **10** started from commercially available D-erythronic-γ-lactone, which was treated with excess benzyl bromide and silver oxide to protect the hydroxyl groups (Scheme 1).[22] The lactone ring was then opened with *O*-*tert*-butylhydroxylamine in the presence of $AlMe_3$ to give alcohol **19**, which was converted into the corresponding bromide **20** using CBr_4 and PPh_3. Coupling to homocysteine through an S_N2 reaction afforded the desired compound **21**. Deprotection of the two benzyl groups proved to be problematic. A variety of reagents/conditions including hydrogenation with Pd/C, tin(IV) chloride,[23] and boron trichloride−dimethyl sulfide complex[24] were ineffective, giving either incomplete debenzylation or unacceptable levels of side reactions. We found that the best reaction condition was boron trichloride in cold CH_2Cl_2,[25] which not only completely removed the two benzyl groups but also cleaved the Boc and the two *tert*-butyl ester groups in the

Scheme 1[a]

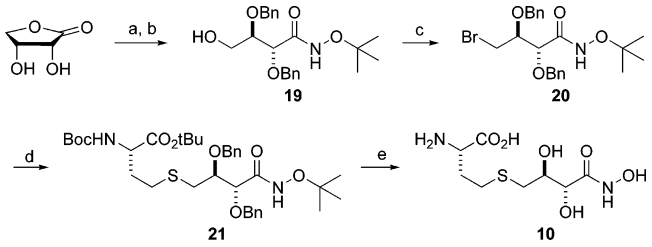

[a] Conditions: (a) BnBr, Ag_2O, Et_2O; (b) H_2NOtBu, $AlMe_3$, DCM; (c) CBr_4, PPh_3, DCM; (d) $BocNHCH(CH_2CH_2SH)CO_2tBu$, LDA, DMF; (e) BCl_3, DCM, −78 °C.

Scheme 2[a]

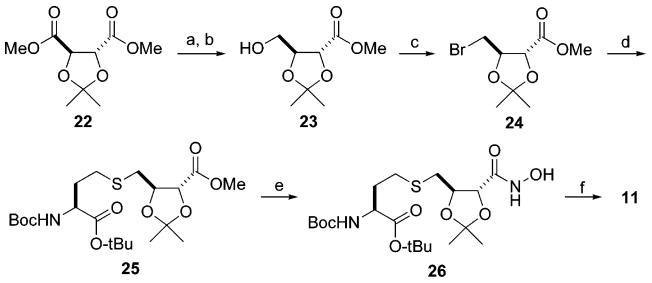

[a] Conditions: (a) KOH, MeOH; (b) BH_3, THF; (c) CBr_4, PPh_3, DCM; (d) $BocHNCH(CH_2CH_2SH)CO_2tBu$, LDA, DMF; (e) H_2NOH, MeOH; (f) TFA, 1 N HCl.

Scheme 3[a]

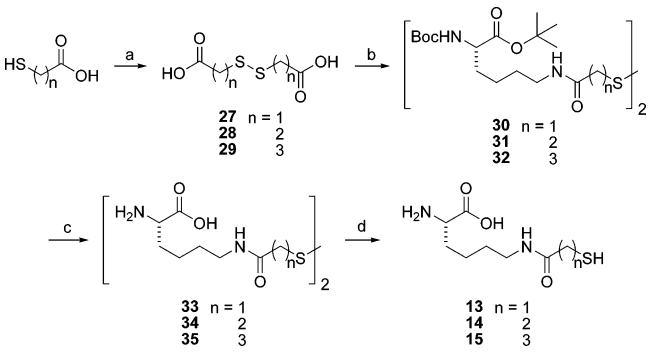

[a] Conditions: (a) H_2O_2, MeOH; (b) N^{α}-Boc-Lys-*O*-*t*Bu, DCC, DMAP; (c) TFA; (d) TCEP.

molecule, all in one step. To prepare compound **11**, commercially available (−)-dimethyl 2,3-*O*-isopropylidene-L-tartrate (**22**) was treated with potassium hydroxide to hydrolyze one of the ester groups (Scheme 2).[26] The resulting monocarboxylic acid was reduced with borane to afford alcohol **23**. The alcohol was converted to bromide **24** with carbon tetrabromide and triphenylphosphine and coupled to Hcys to give methyl ester **25**. Incubation with excess hydroxylamine converted the ester into hydroxamic acid **26**, which was completely deprotected by treatment with TFA and 1 N HCl to afford compound **11**.

Compounds **13**−**15** were prepared from the corresponding mercapto carboxylic acids (Scheme 3). The thiol group was protected by oxidation into disulfide with hydrogen peroxide. The carboxyl group was then reacted with a properly protected lysine derivative to afford compounds **30**−**32**, which were subsequently treated with TFA to generate the corresponding amino acids **33**−**35**. The disulfides in **33**−**35** were reduced to free thiols **13**−**15** by tris(carboxyethyl)phosphine prior to inhibition assays. Compound **16** was synthesized as shown in Scheme 4. N^{α}-Boc-Lys-*O*-*t*Bu was reacted with *p*-methoxybenzaldehyde to form an imine intermediate, which was oxidized

Scheme 4[a]

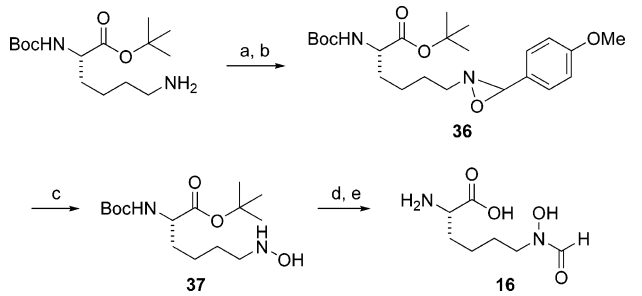

[a] Conditions: (a) $MeOC_6H_4CHO$, Na_2SO_4, DCM; (b) *m*CPBA, DCM; (c) H_2NOH, MeOH; (d) HCO_2H, Ac_2O, DCM; (e) TFA.

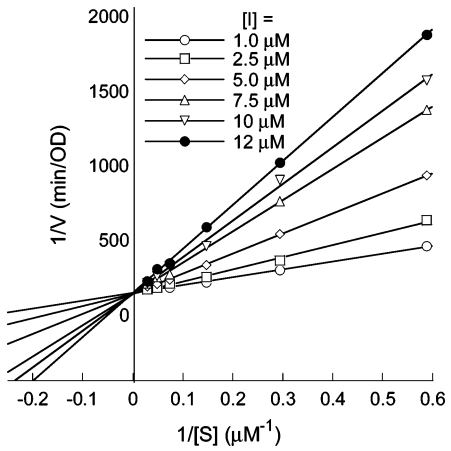

Figure 3. Lineweaver−Burke plot showing the competitive inhibition of Co-BsLuxS by inhibitor **10**.

with *m*-chloroperbenzoic acid to furnish oxaziridine **36**. Treatment of **36** with hydroxylamine produced hydroxylamine **37**. Formylation of the amine followed by TFA deprotection gave the desired compound **16**. *S*-Ribosylcysteine (SRC and compound **18** in Figure 2) was prepared enzymatically by treating commercially available *S*-adenosylcysteine with nucleosidase Pfs. *δ*-Ribosylornithine (compound **17**) was similarly prepared by hydrolyzing the natural product sinefungin with Pfs.

Results and Discussion

Compounds **10**−**12** and **16**−**18** were assayed against Co(II)-substituted *B. subtilis* LuxS (Co-BsLuxS) by using SRH as the substrate and monitoring the release of Hcys with 5,5′-dithiobis-(2-nitrobenzoic acid (DTNB).[27] Compounds **10** and **11** acted as potent, competitive inhibitors (as determined with **10**), with K_I values of 0.72 and 0.37 μM, respectively (Figure 3 and Table 1). The same K_I values were obtained for the native ferrous-containing enzyme Fe-BsLuxS. To our knowledge, these are the most potent LuxS inhibitors that have so far been reported. They are, however, significantly weaker inhibitors against Zn-BsLuxS (20 and 11 μM, respectively). They are also less potent against Co(II)-substituted *Escherichia coli* (Co-EcLuxS) and *V. harveyi* (Co-VhLuxS) LuxS (Table 1). Interestingly, the K_I values roughly correlated with the K_M values of the various enzyme forms (against SRH); the enzymes with higher K_M values also have higher K_I values, suggesting that these compounds are good mimics of LuxS catalytic intermediate(s). Compound **12**, which contains only the ribose portion, binds to LuxS with orders of magnitude lower affinity ($K_I \geq 150$ μM), highlighting the importance of the amino acid moiety to the overall binding affinity. Likewise, methionine binds only weakly to the LuxS active site ($K_I = 61$ μM), indicating that binding

Table 1. Inhibition Constants against LuxS

enzyme		K_I (μM)								K_M (μM)
		10	**11**	**12**	**13**	**14**	**15**	**16**	Met	
BsLuxS	Co	0.72 ± 0.02	0.37 ± 0.04	156 ± 5	132 ± 17	155 ± 24	473 ± 70	68 ± 8	61 ± 2	2.3
	Fe	0.72 ± 0.03	0.43 ± 0.02	147 ± 5	ND[a]	ND	ND	ND	ND	1.9
	Zn	19.6 ± 1.1	10.6 ± 0.4	2400 ± 400	ND	ND	ND	ND	ND	58
EcLuxS	Co	3.2 ± 0.3	12.7 ± 0.4	720 ± 120	ND	ND	ND	ND	ND	16
VhLuxS	Co	9.7 ± 0.4	12.8 ± 0.3	550 ± 20	ND	ND	ND	ND	ND	39

[a] ND = not determined.

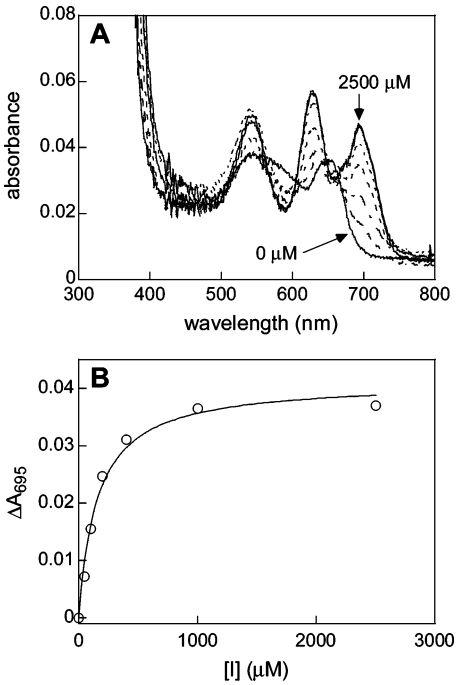

Figure 4. (A) Concentration-dependent spectral changes of Co-BsLuxS in the presence of inhibitor **14**. (B) Secondary plot of absorbance at 695 nm against inhibitor concentration from panel A.

to the metal center is also crucial for high affinity. On the other hand, the similar K_I values of compounds **10** and **11** suggest that the central portion of the inhibitors (and likely substrates and intermediates) are not engaged in specific interactions with the enzyme, as we had anticipated.

Compounds **13**−**15** could not be tested with the DTNB-based activity assay, because they contain free thiols in their structures. Their binding affinity to the LuxS active site was determined by taking advantage of the absorption spectral changes of the Co(II) center upon inhibitor binding. The Co(II) ion is very sensitive to changes to its environment and thus provides a convenient probe for ligand changes associated with inhibitor binding at the metal center.[28] The free enzyme had a broad absorption peak between 500 and 600 nm and a sharper peak at 660 nm (Figure 4A). Addition of thiol **14** caused concentration-dependent spectral changes, resulting in the eventual loss of the above two peaks and the appearance of three sharp bands at 545, 630, and 695 nm. A plot of the absorbance at 695 nm as a function of inhibitor concentration gave a secondary plot as shown in Figure 4B. Curve fitting of the data gave a K_D value of 155 μM for compound **14**. The K_D values of compounds **13** and **15** were similarly determined to be 132 and 473 μM, respectively. The drastic spectral changes suggest that the thiols (and possibly the carbonyl group as well) replaced the metal-bound water in the free enzyme and became directly coordinated with the metal ion. Since the overall affinity is weak, we suspect that the amino acid moiety of these compounds did not fit into the homocysteine-binding pocket. Compound **16**, which has a bidentate *N*-formylhydroxylamine ligand, also exhibited weak inhibition, with a K_I value of 68 μM (Table 1). This K_I value is similar to that of methionine ($K_I = 61$ μM), suggesting that it might bind to the enzyme via its amino acid end. We also synthesized a series of compounds in which the thiol group of cysteine or homocysteine is covalently linked to a hydroxamate moiety via linkers of varying length (R. Liu and D. Pei, unpublished results). These compounds all showed only moderate inhibition of LuxS (K_I values of 15−71 μM).

δ-Ribosylornithine (**17**) and *S*-ribosylcysteine (**18**) were also tested as potential LuxS substrates and/or inhibitors. Compound **17** did not show any significant inhibition against LuxS in the DTNB assay. Prolonged incubation of high concentrations of **17** with Co-BsLuxS also failed to cause any spectral changes. Since the amino acid (ornithine) and ribose are connected through a C−C bond, DPD formation was not expected. Attempts to observe any 2- and/or 3-ketone intermediates by ^{13}C NMR spectroscopy also failed. On the other hand, compound **18** (SRC) acted as a slow substrate of LuxS. Although its reactivity was too low to be quantitatively determined by the DTNB assay, treatment of **18** with LuxS in the presence of 1,2-phenylenediamine resulted in the formation of a quinoxaline derivative, indicating that DPD was released by the enzyme.[16,29,32] When assayed as an inhibitor, SRC exhibited an apparent K_I value of 70 μM.

To gain insight into the structural basis of LuxS inhibition by the above compounds, Co-BsLuxS was cocrystallized with the inhibitors **10** and **11** from a solution of ammonium sulfate at pH 7.0. Crystals of both LuxS complexes are isomorphous with those of the 2-ketone intermediate **4** complex (PDB code 1YCL),[21] and contain a LuxS dimer oriented along a 2-fold crystallographic axis, with one monomer per asymmetric unit. The active site is formed at the dimer interface. The structure with inhibitor **10** was refined at 1.8 Å resolution to an *R* factor of 19.4% and a free *R* factor of 22.6% (Table 2). The final model includes residues 4−157 of LuxS, 1 Co^{2+} ion, 138 water molecules, 2 sulfate ions, and 1 inhibitor molecule. The temperature factors for the protein atoms range from 11 to 45 Å^2, while those for the inhibitor range from 19 to 24 Å^2, indicating full occupancy of the inhibitor. The Cα atoms of the structures of LuxS bound to **10** and 2-ketone intermediate **4** can be superimposed to an rmsd of 0.2 Å. There are no significant conformational changes in LuxS, even for side chains of residues at the active site.

Clear electron density for inhibitor **10** allowed for it to be fit into the model unambiguously (Figure 5). Inhibitor **10** is bound to LuxS in a manner very similar to that of 2-ketone intermediate **4** (Figure 5C,E and Table 3). A significant difference lies in the interaction with the metal ion. While intermediate **4** binds monodentately to the metal ion via its C2 carbonyl oxygen, inhibitor **10** interacts with the Co^{2+} ion bidentately, through the oxygen atoms of both C2 carbonyl and C3 hydroxyl groups (metal−oxygen distances of 2.2 and 2.3 Å, respectively). The hydroxamate oxygen atom O1 is hydrogen bonded to the side chains of Arg-39 and His-11. The O1 atom does not however

Table 2. Data Collection and Refinement Statistics

data collection	inhibitor **10**	inhibitor **11**
space group	$P6_522$	$P6_522$
a, *b* (Å)	62.9	62.8
c (Å)	148.6	148.6
resolution (Å)	20.4−1.8	27.2−1.9
no. of reflns	89103	97262
no. of unique reflns	15675	14925
completeness (%)	91.4 (54.5)[a]	98.6 (90.6)
redundancy	5.5 (1.4)	5.9 (1.2)
R_{merge}[b]	6.2 (20.3)	5.2 (18.4)
I/σ[c]	17.2 (3.9)	22 (5.1)
Refinement		
resolution (Å)	20.4−1.8	27.2−1.9
no. of reflns (working/free)	14054/1568	13382/1500
completeness (%)	91.1	98.6
mean *B* factor (Å^2)	21.1	19.6
estimated coordinate error[d]	0.17	0.16
R factor	19.4 (26.8)	19.1 (22.1)
R_{free}[e] (%)	22.6 (32.2)	22.1 (26.1)
no. of water molecules	138	130
RMSD(bonds) (Å)	0.004	
RMSD(angles) (deg)	1.2	

[a] Numbers in parentheses refer to the highest shell only. [b] $R_{merge} = \sum|I_h - \langle I\rangle_h|/\sum I_h$, where $\langle I\rangle_h$ is the average intensity over symmetry equivalents. [c] I/σ is the mean of the intensity/sigma of the unique, averaged reflections. [d] The estimated coordinate error is the value from the cross-validated σ plot. [e] *R* factor $= \sum|F_{obsd} - F_{calcd}|/\sum_{obsd}$. R_{free} is calculated from 10% of the reflections that are omitted from the refinement.

interact directly with Ser-6, as was observed in the LuxS−ketone **4** complex, due to a change in the N1−C2 torsion angle imposed by its partial double bond character. The sulfhydryl group of catalytic residue Cys-84, which was replaced by alanine in the complex with intermediate **4**, is proximal to the N1 (3.4 Å), C2 (3.5 Å), and C3 (4.1 Å) atoms of the inhibitor (Table 2). This is consistent with Cys-84 serving as a proton donor and acceptor to (and from) these atoms during the course of catalysis, as outlined in Figure 1. The C3 hydroxyl (O3) is hydrogen bonded to Glu-57, consistent with the role of Glu-57 as a general base during the carbonyl migration reactions (Figure 1). The C4 hydroxyl (O4) is hydrogen bonded to the Ser-6 side chain. The atoms of the homocysteine portion of the inhibitor are bound essentially the same as observed for the ketone **4** complex. Interestingly, a well-ordered water molecule, near the O2 atom of inhibitor **10** and forming hydrogen bonds with Ser-6 and His-11, is observed in both structures. Given the proximity of this water to the reactive groups of the protein and the inhibitor, it could conceivably have an important role during catalysis, presumably facilitating proton-transfer reactions.

The structure of Co-BsLuxS was also determined in complex with inhibitor **11**, and refined at 1.9 Å resolution to an *R* factor of 19.1% and a free *R* factor of 22.2% (Table 2 and Figure 5D). The electron density allowed for all atoms of inhibitor **11** to be placed in the structure unambiguously. Inhibitor **11** differs from inhibitor **10** only in having an inverted stereochemical configuration at the C4 position. This change is evident in the electron density map, although the density for the C4 and O4 atoms is slightly weaker than for the rest of the compound, indicating a higher degree of flexibility. Due to the change in configuration, the O4 atom of inhibitor **11** points down (as viewed in Figure 5D), and is closer to the Co^{2+} atom (3.5 Å) than is the case for the O4 atom of inhibitor **10** (5.2 Å). Thus, the structure of the complex with inhibitor **11** demonstrates that LuxS binds to substrate-related compounds with some degree of conformational variation at the C4 position. In comparing the structures of Co-BsLuxS bound to inhibitors **10**, **11**, and intermediate **4**, it is apparent that LuxS binds to substrate-related

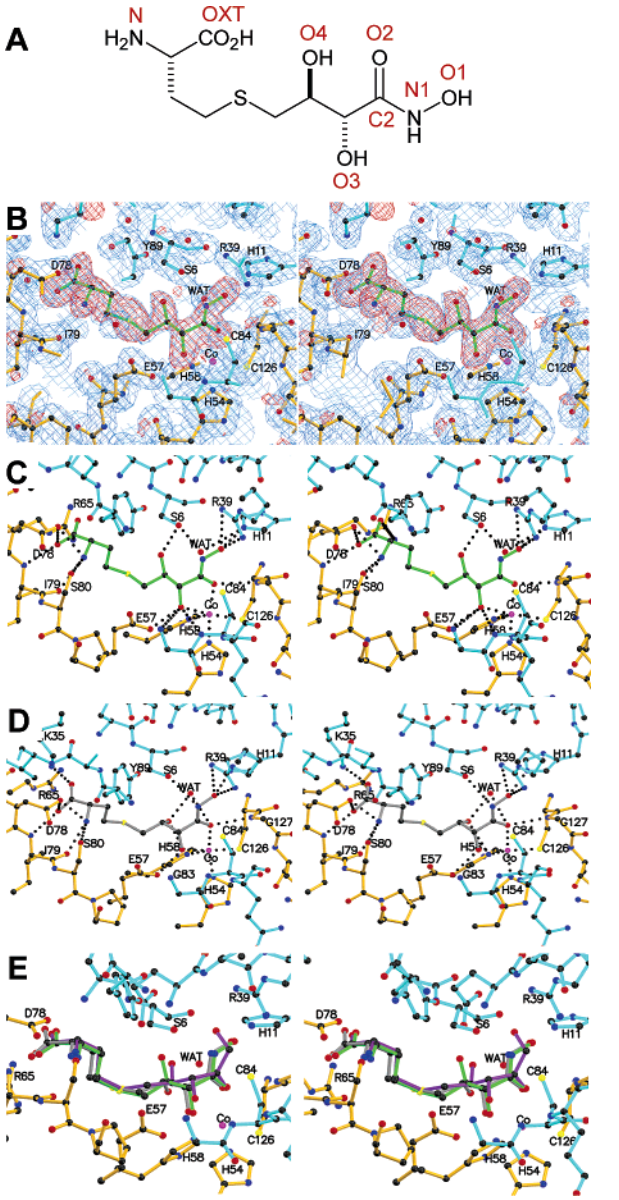

Figure 5. Structure of Co-BsLuxS in complex with inhibitors **10** and **11**. The two subunits of LuxS are colored gold and cyan, and the Co^{2+} ion is colored magenta. (A) Designation of atoms and groups in inhibitor **10** (according to atom numbering in SRH). (B) Stereoview of the electron density for inhibitor **10**. The blue cage is the 1.8 Å $2F_{obsd} - F_{calcd}$ electron density map contoured at 1σ. The red cage is an $F_{obsd} - F_{calcd}$ map, contoured at 2.5σ, calculated before the inhibitor was added to the model. The inhibitor is shown with green bonds. (C) Stereoview showing hydrogen-bonding interactions between LuxS and inhibitor **10** as dotted lines. (D) Stereoview showing the hydrogen-bonding interactions in the structure of Co-BsLuxS in complex with inhibitor **11** (gray bonds). Notice that the stereochemical configuration at the C4 position is inverted relative to that of inhibitor **10** in panel C, causing the O4 atom to point down, in the direction of the Co^{2+} atom. (E) Stereoview of a superposition of the structures of inhibitors **10** (green), **11** (gray), and 2-ketone intermediate **4** (magenta) in complex with Co-BsLuxS. The superposition is based on the protein atoms, which are shown only for the structure of LuxS in complex with inhibitor **10**, but are virtually identical in the other two structures. Notice that the O2 and O3 atoms form very similar interactions with the Co^{2+} ion in the three structures.

compounds with a virtually fixed conformation for the homocysteine portion, and a more adaptable conformation for the functional groups of the ribosyl portion, as would be predicted from the reaction scheme in Figure 1. This suggests that, in

Table 3. Atomic Interactions between LuxS and Inhibitors **10** and **11**[a]

inhibitor atom	LuxS atom	**10**	**11**
N1	Cys-84 SG	3.4	3.5
O1	His-11 NE2	2.7	2.6
O1	Arg-39 NH1	3.2	3.4
O1	Arg-39 NH2	2.8	3.1
O1	Gly-127 N	3.5	3.4
C2	Cys-84 SG	3.5	3.6
O2	Co^{2+}	2.2	2.1
O2	water	3.1	3.2
O3	Co^{2+}	2.3	2.3
O3	Glu-57 OE1	2.6	2.7
O3	His-58 NE2	3.0	3.0
O4	Ser-6 OG	2.5	3.7
N	Asp-78 OD1	2.9	2.9
N	Ile-79 O	2.8	2.8
N	Ser-80 OG	3.3	3.3
OXT	Asp78 OD1	3.2	3.3
OXT	Ile-79 N	3.0	3.1

[a] Distances in angstroms. In the LuxS−**10** complex, the number of water molecules was 469, and in LuxS−**11**, it was 448.

designing future generations of LuxS inhibitors, one may be able to employ a wide variety of linker structures to connect the amino acid and metal-chelating moieties. A conformationally constrained linker should be particularly effective.

It is worth noting that both inhibitors **10** and **11** coordinate with the metal ion using the O2 and O3 atoms, instead of bidentate interaction via the hydroxamate (O1 and O2), as we had anticipated (Figure 2A). One possible reason for this is that binding via O1 and O2 would eliminate stable hydrogen-bonding interactions with Arg-39 and His-11. Alternatively, geometric constraints exerted by locking the homocysteine moiety into its binding pocket may prevent the planar hydroxamate from approaching the metal ion at an optimal distance/angle. This latter point may have important implications in LuxS catalytic mechanism. The planar hydroxamate closely mimics the enediolate intermediates, whose tighter binding to the metal ion would slow or prevent catalytic turnover.

Conclusion

A series of LuxS substrate and intermediate analogues have been synthesized and tested. This effort has led to the first submicromolar inhibitors against this enzyme. The cocrystal structures of LuxS bound with inhibitors **10** and **11** revealed that a high-affinity inhibitor should be able to bind to both the homocysteine-binding pocket and the metal ion and suggested possible strategies for designing future generations of LuxS inhibitors. The structures also provided additional evidence for the proposed roles of active-site residues (e.g., Glu-57 and Cys-84 as general acids/bases) during catalysis.

Experimental Section

General Procedures. Pfs and Co^{2+}-, Zn^{2+}-, or Fe^{2+}-substituted LuxS from *B. subtilis*, *E. coli*, and *V. harveyi* were overexpressed in *E. coli* and purified to apparent homogeneity as described previously.[16] All chemicals and reagents were purchased from Sigma-Aldrich (St. Louis, MO). Unless otherwise noted, materials were obtained from commercial suppliers and used without further purification. Triethylamine was dried under KOH; tetrahydrofuran (THF), dichloromethane, and diethyl ether were treated with the SOLV-TEK solvent purification system (Berryville, VA). DMF was dried with molecular sieves. ^{1}H and ^{13}C NMR spectra were obtained on a 400 or 250 MHz Bruker NMR spectrometer. Unless otherwise indicated, all NMR data were collected at room temperature in $CDCl_3$ with internal $CHCl_3$ as reference (7.26 ppm for ^{1}H and 77.23 ppm for ^{13}C), DMSO-d_6 with internal DMSO as reference (2.49 ppm for ^{1}H and 39.70 ppm for ^{13}C), CD_3OD with internal CH_3OH as reference (3.30 ppm for ^{1}H and 49.00 ppm for ^{13}C), and D_2O with H_2O as reference (4.63 ppm for ^{1}H). Analytical thin-layer chromatography (TLC) was carried out on commercial silica gel 60 plates, 0.25 thickness, with a fluorescent indicator (F-254). Visualization was accomplished by UV light, staining with 5% phosphomolybdic acid in ethanol, or staining with $KMnO_4$ in an aqueous solution of sodium carbonate. Column chromatography was performed with 32−63 μm silica gel. Solvents for chromatography were reagent grade and used as received. Mass spectra were performed with positive ion electrospray ionization or negative ion electrospray ionization.

(2*R*,3*R*)-2,3-Bis(benzyloxy)-*N*-*tert*-butoxy-4-hydroxybutyramide (19). To a solution of *O*-*tert*-butylhydroxylamine hydrochloride (300 mg, 2.39 mmol) in CH_2Cl_2 (17 mL) was added a 2 M solution of $AlMe_3$ in hexanes (1.12 mL, 2.24 mmol) at 0 °C, followed by the addition of d-3,4-dibenzylerythronic-γ-lactone (479 mg, 1.61 mmol), which had been prepared from d-erythronic-γ-lactone according to a literature method.[22] The reaction mixture was heated to reflux for 20 h. A saturated solution of NH_4Cl in water was added to quench the excess $AlMe_3$, and the mixture was extracted with $CHCl_3$ (5 × 25 mL). The organic phase was combined, dried over $MgSO_4$, concentrated, and purified by silica gel chromatography (1:1 EtOAc/hexanes) to afford **19** as a white solid (494 mg, 79% yield, R_f = 0.35). ^{1}H NMR (400 MHz, DMSO-d_6): δ 10.55 (s, 1H), 7.34−7.24 (m, 10H), 4.63 (d, J = 12.0 Hz, 1H), 4.55 (d, J = 12.0 Hz, 1H), 4.49 (d, J = 11.6 Hz, 1H), 4.42 (d, J = 12.0 Hz, 1H), 3.96 (d, J = 6.4 Hz, 1H), 3.74−3.70 (m, 1H), 3.68−3.65 (m, 1H), 3.54 (quintet, J = 6.4 Hz, 1H), 1.14 (s, 9H). ^{13}C NMR (100 MHz, DMSO-d_6): δ 167.7, 138.6, 137.9, 128.2, 127.9, 127.5 (d), 127.2, 80.8, 80.3, 77.1, 71.6, 71.3, 60.0, 26.4. HRESI-MS: m/z calcd for $C_{22}H_{29}NO_5Na^+$ (M + Na^+) 410.1938, found 410.1943.

(2*R*,3*S*)-2,3-Bis(benzyloxy)-*N*-*tert*-butoxy-4-bromobutyramide (20). To a solution of alcohol **19** (468 mg, 1.21 mmol) in CH_2Cl_2 (12 mL) were added triphenylphosphine (387 mg, 1.47 mmol) and carbon tetrabromide (481 mg, 1.45 mmol) in an ice bath. The solution was kept under an argon atmosphere and stirred overnight at room temperature. The solvent was then removed by rotary evaporation, and the residue was purified by silica gel chromatography (1:3 EtOAc/hexanes) to give **20** as a white solid (471 mg, 87% yield, R_f = 0.32). ^{1}H NMR (400 MHz, $CDCl_3$): δ 8.40 (s, 1H), 7.37−7.30 (m, 10H), 4.74 (d, J = 11.2 Hz, 1H), 4.68−4.63 (m, 3H), 4.19 (d, J = 3.2 Hz, 1H), 4.10−4.06 (m, 1H), 3.64−3.55 (m, 2H), 1.22 (s, 9H). ^{13}C NMR (100 MHz, $CDCl_3$): δ 167.8, 137.4, 136.6, 128.7, 128.4 (d), 128.1 (d), 128.0, 82.5, 80.0, 79.2, 77.2, 73.6, 73.3, 31.0, 26.3. HRESI-MS: m/z calcd for $C_{22}H_{28}BrNO_4Na^+$ (M + Na^+) 472.1094, found 472.1097.

***tert*-Butyl (2*S*)-4-[(2*R*,3*S*)-2,3-Bis(benzyloxy)-3-*tert*-butoxycarbamoylpropylmercapto]-2-*tert*-butoxycarbonylaminobutyrate (21)**. Freshly prepared L-BocNHCH(CH_2CH_2SH)CO_2tBu[29] (52 mg, 0.18 mmol) was dissolved in anhydrous DMF (0.4 mL), and the solution was purged with argon for 10 min. A 1.5 M solution of LDA in cyclohexane (0.36 mL, 0.54 mmol) was added to the above solution cooled in an ice−water bath. This solution was stirred at 0 °C for 10 min and mixed with a solution of bromide **20** (84 mg, 0.19 mmol) in dry DMF (1 mL). This reaction mixture was stirred at room temperature for 2 days. The solvent was removed by rotary evaporation, and the yellow residue was suspended in a saturated NH_4Cl solution and extracted with EtOAc (3 × 10 mL). The organic phase was dried over $MgSO_4$, concentrated, and purified by column chromatography (1:3 EtOAc/hexanes) to provide **21** as a pale yellow gel (42 mg, 36% yield, R_f = 0.16). ^{1}H NMR (400 MHz, $CDCl_3$): δ 8.64 (s, 1H), 7.38−7.27 (m, 10H), 5.22 (br d, J = 7.6 Hz, 0.8H), 4.65 (d, J = 11.2 Hz, 4H), 4.25−4.24 (m, 2H), 4.02−3.98 (m, 1H), 2.81 (dd, J = 14.0 Hz, 6.8 Hz, 1H), 2.72 (dd, J = 14.0 Hz, 5.6 Hz, 1H), 2.60−2.49 (m, 2H), 2.04−2.00 (m, 1H), 1.87−1.80 (m, 1H), 1.45 (s, 9H), 1.44 (s, 9H), 1.23 (s, 9H). ^{13}C NMR (100 MHz, $CDCl_3$): δ 171.7, 168.4, 155.6, 138.0, 137.2, 128.8, 128.3 (d), 128.1 (d), 127.9, 82.5, 82.2, 80.1, 80.0 (d), 73.5 (d), 53.5, 32.9 (d), 29.1, 28.6, 28.2, 26.5.

HRESI-MS: *m/z* calcd for $C_{35}H_{52}N_2O_8SNa^+$ (M + Na^+) 683.3337, found 683.3336.

(2*S*)-2-Amino-4-[(2*R*,3*S*)-2,3-dihydroxy-3-*N*-hydroxycarbamoylpropylmercapto]butyric Acid (10). A solution of 1 M BCl_3 in CH_2Cl_2 (0.50 mL, 0.50 mmol) was charged into a 10 mL round-bottom flask and cooled to −78 °C, and compound **21** (53 mg, 0.080 mmol) in CH_2Cl_2 (0.72 mL) was added dropwise at −78 °C. The yellow reaction mixture was stirred at −78 °C for 3 h. MeOH/CH_2Cl_2 (2:1, 1.08 mL) was then added at −78 °C, and the mixture was stirred for another 5 min. The solvent was removed by rotary evaporation, and 2 mL of MeOH was added and then removed by rotary evaporation. The residue was purified by silica gel chromatography (30% H_2O in CH_3CN) to give product **4** as a white gel (15 mg, 71% yield, R_f = 0.34). The product was further purified by affinity chromatography with Affi-Gel boronate gel (Bio-Rad), which was eluted with 30 mM Na_2HPO_4−NaH_2PO_4 buffers of the following pH values: 8.5, 8.1, 7.6, 7.0, 6.75, 6.5, 6.25, 6.0, 5.5, 5.0, and 4.5. Compound **4** was collected over the pH range of 6.5−6.0. ^{1}H NMR (400 MHz, D_2O): δ 4.09 (d, J = 4.4 Hz, 1H), 3.86 (quintet, J = 4.4 Hz, 1H), 3.68 (t, J = 6.0 Hz, 1H), 2.65 (dd, J = 14.0 Hz, 4.0 Hz, 1H), 2.58−2.51 (m, 3H), 2.02−1.92 (m, 2H). ^{13}C NMR (100 MHz, D_2O): δ 174.2, 170.1, 72.8, 71.1, 53.9, 33.0, 30.3, 27.4. HRESI-MS: *m/z* calcd for $C_8H_{15}N_2O_6S^-$ (M − H^-) 267.0651, found 267.0656.

Methyl (4*R*,5*S*)-5-Hydroymethyl-2,2-dimethyl[1,3]dioxolane-4-carboxylate (23). To a solution of dimethyl (−)-2,3-*O*-isopropylidene-L-tartrate **(22)** (0.95 mL, 5.0 mmol) in MeOH (25 mL) was added 85% KOH pellet (0.33 g, 5.0 mmol). The solution was stirred overnight at rt under an argon atmosphere. The solvent was removed by rotary evaporation, and the residue was kept under high vacuum for 3 h. The resultant white solid was mixed with anhydrous THF (9.8 mL) and treated with 1 M BH_3 in THF solution (6.5 mL, 6.5 mmol) in an ice−water bath. The reaction mixture was stirred for 8 h. Saturated $NaHCO_3$ solution was slowly added to the above mixture until bubbling stopped. The solvent was removed by rotary evaporation, and the remaining aqueous phase was extracted with EtOAc (100 mL). The organic phase was dried over $MgSO_4$ and concentrated. The residue was purified by silica gel chromatography (1:1 EtOAc/hexanes) to provide **23** as a colorless oil (0.34 g, 36% yield over two steps, R_f = 0.29). ^{1}H NMR (400 MHz, $CDCl_3$): δ 4.48 (d, J = 7.6 Hz, 1H), 4.27−4.23 (m, 1H), 3.96 (dd, J = 12.4 Hz, 3.2 Hz, 1H), 3.81 (s, 3H), 3.76 (dd, J = 12.4 Hz, 3.2 Hz, 1H), 1.91 (br s, 0.8H), 1.50 (s, 3H), 1.48 (s, 3H).

Methyl (4*R*,5*R*)-5-Bromomethyl-2,2-dimethyl[1,3]dioxolane-4-carboxylate (24). To a solution of alcohol **23** (279 mg, 1.47 mmol) in CH_2Cl_2 (15 mL) were added triphenylphosphine (0.40 g, 1.53 mmol) and carbon tetrabromide (0.51 g, 1.53 mmol) in an ice−water bath. The solution was stirred overnight at rt under argon. The solvent was removed by rotary evaporation, and the residue was purified by column chromatography (1:3 EtOAc/hexanes) to give **24** as a colorless oil (0.23 g, 62% yield, R_f = 0.47). ^{1}H NMR (250 MHz, $CDCl_3$): δ 4.45−4.38 (m, 2H), 3.81 (s, 3H), 3.70−3.64 (ABm, 1H), 3.60−3.54 (ABm, 1H), 1.52 (s, 3H), 1.46 (s, 3H).

Methyl (4*R*,5*R*)-5-[(3*S*)-3-*tert*-Butoxycarbonyl-3-*tert*-butoxycarbonylaminopropylsulfanylmethyl]-2,2-dimethyl[1,3]dioxolane-4-carboxylate (25). Freshly prepared l-BocNHCH(CH_2CH_2SH)-CO_2tBu[29] (142 mg, 0.48 mmol) was dissolved in dry DMF (2.5 mL), and the solution was purged with argon for 10 min and chilled in an ice−water bath. A 1.5 M solution of LDA in cyclohexane (0.6 mL, 0.9 mmol) was added, and the resulting solution was stirred at 0 °C for 10 min, followed by the addition of bromide **24** (129 mg, 0.51 mmol) in DMF (1.5 mL). This reaction mixture was stirred at rt for 2 days. The solvent was then removed by rotary evaporation, and the yellow residue was suspended in saturated NH_4Cl solution and extracted with EtOAc (3 × 10 mL). The organic layer was dried over $MgSO_4$, concentrated, and purified by silica gel chromatography (1:3 EtOAc/hexanes) to afford **25** as a colorless semisolid (111 mg, 50% yield, R_f = 0.32). ^{1}H NMR (400 MHz, $CDCl_3$): δ 5.08 (br d, J = 7.2 Hz, 0.8H), 4.37−4.32 (m, 2H), 4.25−4.24 (m, 1H), 3.78 (s, 3H), 2.94 (dd, J = 14.4 Hz, 3.6 Hz, 1H), 2.78 (dd, J = 14.4 Hz, 1.6 Hz, 1H), 2.72−2.59 (m, 2H), 2.09−2.06 (m, 1H), 1.93−1.84 (m, 1H), 1.48 (s, 3H), 1.46 (s, 9H), 1.43 (s, 12H). ^{13}C NMR (100 MHz, $CDCl_3$): δ 171.3, 170.8, 155.3, 111.5, 82.1, 79.8, 79.0, 77.9, 53.4, 52.5, 34.4, 33.0, 28.7, 28.3, 28.0, 27.0, 25.8. HRESI-MS: *m/z* calcd for $C_{21}H_{37}NO_8SNa^+$ (M + Na^+) 486.2132, found 486.2121.

***tert*-Butyl (2*S*)-2-*tert*-Butoxycarbonylamino-4-{(4*R*,5*R*)-5-*N*-hydroxycarbamoyl-2,2-dimethyl[1,3]dioxolan-4-ylmethylmercapto}butyrate (26)**. To a solution of ester **25** (63 mg, 0.14 mmol) in MeOH (1 mL) cooled in icy water were added hydroxylamine hydrochloride (40 mg, 0.55 mmol) and 85% KOH (40 mg, 0.61 mmol). This reaction mixture was stirred at rt for 36 h. The solvent was removed under reduced pressure, and the white residue was suspended in water. The aqueous mixture was carefully adjusted to pH ≈ 5 with 1 N HCl and extracted with $CHCl_3$ (3 × 10 mL). The organic phase was concentrated and purified by silica gel chromatography (1:1 EtOAc/hexanes) to produce **26** as a colorless semisolid (44 mg, 70% yield, R_f = 0.25). ^{1}H NMR (400 MHz, $CDCl_3$): δ 9.22 (br s, 0.8H), 5.62 (br s, 0.2H), 5.18 (br m, 0.7H), 4.28−4.14 (m, 2H), 3.95 (br s, 0.3H), 3.22−3.04 (ABm, 1H), 2.80−2.64 (ABm, 1H), 2.65−2.64 (m, 2H), 2.08−2.04 (m, 1H), 1.89−1.88 (m, 1H), 1.46 (s, 12H), 1.44 (s, 12H). ^{13}C NMR (100 MHz, $CDCl_3$): δ 171.4, 167.4, 155.5, 111.3, 82.2, 79.9, 79.5, 53.5, 34.2, 33.0, 28.7, 28.3, 28.0, 27.0, 26.0. HRESI-MS: *m/z* calcd for $C_{20}H_{36}N_2O_8SNa^+$ (M + Na^+) 487.2085, found 487.2075.

(2*S*)-2-Amino-4-[(2*R*,3*R*)-2,3-dihydroxy-3-*N*-hydroxycarbamoylpropylmercapto]butyric Acid (11). Compound **26** (42 mg, 0.09 mmol) was dissolved in 1 mL of TFA, and the solution was stirred at rt for 1 h. TFA was removed by rotary evaporation, and the remaining residue was treated with 1 N HCl for 4 h at rt. The mixture was concentrated, and the crude product was purified on a silica gel column eluted with 30% H_2O in CH_3CN to produce a white solid (24 mg, quantitative yield, R_f = 0.34). ^{1}H NMR (400 MHz, D_2O): δ 4.25 (d, J = 2.8 Hz, 1H), 4.02−3.98 (m, 1H), 3.79−3.76 (m, 1H), 2.75−2.67 (m, 2H), 2.64 (t, J = 7.6 Hz, 2H), 2.15−2.00 (m, 2H). ^{13}C NMR (100 MHz, D_2O): δ 174.1, 170.9, 72.0, 70.6, 53.8, 33.6, 30.3, 27.2. HRESI-MS: *m/z* calcd for $C_8H_{15}N_2O_6S^-$ (M − H^+) 267.0651, found 267.0628.

D-**Erythronohydroxamic Acid (12).** This compound was synthesized according to a literature procedure.[31]

(2*S*)-2-Amino-6-{2-[(5*S*)-5-amino-5-carboxypentylcarbamoylmethyldithio]acetylamino}hexanoic Acid (33). To a solution of 2-mercaptoacetic acid (14 μL, 0.20 mmol) in MeOH (0.5 mL) was added H_2O_2 (20 μL, 0.18 mmol). The mixture was stirred for 1 h at rt, and the solvent was evaporated. The white solid obtained was kept under high vacuum for 6 h and mixed with l-N^{α}-Boc-Lys-*O*-*t*Bu (61 mg, 0.20 mmol), followed by the addition of CH_2Cl_2 (1.5 mL), dicyclohexylcarbodiimide (42 mg, 0.21 mmol), and (dimethylamino)pyridine (24 mg, 0.20 mmol). The reaction mixture was stirred under argon for 18 h at rt. The mixture was filtered, and the white precipitate was rinsed with EtOAc. The filtrate was pooled, concentrated, and treated with TFA (0.8 mL) for 30 min. After rotary evaporation of TFA, the residue was washed with $CHCl_3$ and purified by silica gel chromatography (eluted with 30% H_2O in CH_3CN) to afford **33** as a white solid (13 mg, 30% yield, R_f = 0.23). ^{1}H NMR (400 MHz, D_2O): δ 3.60 (t, J = 6.4 Hz, 2H), 3.34 (s, 4H), 3.14 (t, J = 6.8 Hz, 4H), 1.78−1.68 (m, 4H), 1.51−1.44 (m, 4H), 1.36−1.26 (m, 4H). ^{13}C NMR (100 MHz, D_2O): δ 174.8, 171.4, 54.7, 41.0, 39.5, 30.1, 28.0, 21.8. HRESI-MS: *m/z* calcd for $C_{16}H_{30}N_4O_6S_2Na^+$ (M + Na^+) 461.1504, found 461.1472.

(2*S*)-2-Amino-6-{3-[2-(5*S*)-5-amino-5-carboxypentylcarbamoylethyldithio]propionylamino}hexanoic Acid (34). This compound was prepared in a manner similar to that of compound **33**. ^{1}H NMR (400 MHz, D_2O): δ 3.59 (t, J = 6.0 Hz, 2H), 3.08 (t, J = 6.8 Hz, 4H), 2.83 (t, J = 6.8 Hz, 4H), 2.54 (t, J = 6.8 Hz, 4H), 1.78−1.70 (m, 4H), 1.45−1.37 (m, 4H), 1.31−1.25 (m, 4H). ^{13}C NMR (100 MHz, D_2O): δ 174.7, 174.1, 54.7, 39.0, 35.0, 33.4, 30.1, 28.0, 27.1, 21.8. HRESI-MS: *m/z* calcd for $C_{18}H_{34}N_4O_6S_2Na^+$ (M + Na^+) 489.1812, found 489.1801.

(2*S*)-2-Amino-6-{4-[3-(5*S*)-5-amino-5-carboxypentylcarbamoylpropyldithio]butyrylamino}hexanoic Acid (35). This compound

was prepared in a manner similar to that of **33**. ^{1}H NMR (400 MHz, D_2O): δ 3.67 (t, J = 6.0 Hz, 2H), 3.13 (t, J = 6.8 Hz, 4H), 2.68 (t, J = 6.8 Hz, 4H), 2.43−2.28 (m, 4H), 2.09−1.91 (m, 4H), 1.85−1.77 (m, 4H), 1.52−1.37 (m, 4H), 1.35−1.28 (m, 4H). ^{13}C NMR (100 MHz, D_2O): δ 175.9, 174.8, 54.7, 38.9, 37.1, 34.3, 30.1, 28.7, 28.0, 24.7, 21.8. HRESI-MS: *m*/*z* calcd for $C_{20}H_{38}N_4O_6S_2Na^+$ (M + Na^+) 517.2125, found 517.2105.

***tert*-Butyl (2*S*)-2-*tert*-Butoxycarbonylamino-6-[3-(4-methoxyphenyl)oxaziridin-2-yl]hexanoate (36).** To a solution of L-N^{α}-Boc-Lys-*t*Bu (0.18 g, 0.60 mmol) in CH_2Cl_2 (6 mL) were added 4-methoxybenzadehyde (78 μL, 0.63 mmol) and Na_2SO_4 (0.84 g, 5.9 mmol). The reaction mixture was stirred at rt for 16 h under an argon atmosphere. The mixture was filtered, and the solid was washed with EtOAc. The filtrate was concentrated under reduced pressure to give a yellow oil. The oil was dissolved in CH_2Cl_2 (3 mL) and mixed with *m*-chloroperbenzoic acid (141 mg, 0.63 mmol) dissolved in CH_2Cl_2 (3 mL) at −78 °C. The reaction mixture was stirred overnight at rt and under argon. Saturated $NaHCO_3$ solution was added, and the mixture was extracted with CH_2Cl_2 (3 × 20 mL). The organic phase was combined, dried over $MgSO_4$, and concentrated. The crude product was purified by silica gel chromatography (15% EtOAc in hexane) to give a colorless oil (126 mg, 48% yield over two steps, R_f = 0.13). ^{1}H NMR (400 MHz, $CDCl_3$): δ 7.31 (d, J = 8.4 Hz, 2H), 6.88 (d, J = 8.0 Hz, 2H), 5.04 (d, J = 7.6 Hz, 1H), 4.42 (s, 1H), 4.18−4.13 (m, 1H), 3.79 (s, 3H), 3.00−2.94 (m, 1H), 2.70−2.65 (m, 1H), 1.81−1.59 (m, 6H), 1.44 (s, 9H), 1.43 (s, 9H). ^{13}C NMR (100 MHz, $CDCl_3$): δ 172.1, 161.2, 155.6, 129.1, 127.0, 114.1, 82.0, 80.5 (d), 79.8, 61.9 (d), 55.5, 54.0, 33.0 (d), 28.5, 28.2, 27.8, 23.2 (d).

***tert*-Butyl (2*S*)-2-*tert*-Butoxycarbonylamino-6-hydroxyaminohexanoate (37).** To a mixture of compound **36** (126 mg, 0.29 mmol) in MeOH (3 mL) was added hydroxylamine hydrochloride (31 mg, 0.43 mmol). The reaction mixture was stirred under argon gas for 12 h at rt. After rotary evaporation of the solvent, the residue was extracted with EtOAc/H_2O. The aqueous phase was adjusted to pH $\approx$ 7 with a saturated $NaHCO_3$ solution and extracted with CH_2Cl_2 (3 × 20 mL). The CH_2Cl_2 solution was combined, dried over $MgSO_4$, and concentrated. The crude product was purified by silica gel chromatography with EtOAc and then 10% MeOH in EtOAc as eluent to give a colorless oil (54 mg, 59% yield, R_f = 0.54). ^{1}H NMR (400 MHz, $CDCl_3$): δ 5.14 (d, J = 8.0 Hz, 1H), 4.17−4.13 (m, 1H), 2.95−2.85 (m, 2H), 1.81−1.48 (m, 6H), 1.45 (s, 9H), 1.43 (s, 9H). ^{13}C NMR (100 MHz, $CDCl_3$): δ 172.3, 155.7, 82.0, 79.9, 53.9, 53.7, 33.1, 28.5, 28.2, 26.7, 23.8.

(2*S*)-2-Amino-6-(*N*-formyl-*N*-hydroxylamino)hexanoic Acid (16). To ice-cooled Ac_2O was added dropwise formic acid, and the mixture was stirred for 10 min in the ice bath. The mixture was then warmed to 50 °C, stirred for another 5 min, and chilled again in the ice−water bath. A solution of compound **37** (54 mg, 0.17 mmol) in CH_2Cl_2 (1.5 mL) was added dropwise. The reaction mixture was stirred for 13 h at rt under an argon atmosphere. The solution was washed with saturated $NaHCO_3$ and the 1 N HCl solutions. The organic layer was dried over $MgSO_4$ and concentrated. The residue was treated with TFA (1 mL) for 40 min. TFA was removed by rotary evaporation and high vacuum. The crude product was washed with $CHCl_3$ six times and purified by silica gel chromatography (30% H_2O in CH_3CN as eluent) to afford a white solid (10 mg, 77% yield). ^{1}H NMR (400 MHz, D_2O): δ 7.81 (s, 1H), 3.61 (t, J = 6.0 Hz, 1H), 3.49−3.43 (m, 2H), 1.78−1.74 (m, 2H), 1.62−1.55 (m, 2H), 1.30−1.21 (m, 2H). ^{13}C NMR (100 MHz, D_2O): δ 174.7, 163.6, 54.6, 50.2, 29.9, 25.8, 21.2. HRESI-MS: *m*/*z* calcd for $C_7H_{14}N_2O_4Na^+$ (M + Na^+) 213.0851, found 213.0868.

***δ*-Ribosylornithine (17) and *S*-Ribosylcysteine (18).** Compounds **17** and **18** were prepared by treating sinefungin and *S*-adenosylcysteine (10 mM), respectively, with recombinant nucleosidase Pfs[16] (10 μM) in a buffer containing 50 mM HEPES (pH 7.0) and 150 mM NaCl for 2 h at room temperature. The reaction progress was monitored spectrophotometrically on the basis of the absorption difference between adenosine and adenine ($\Delta\epsilon_{276}$ = −1.4 mM^{-1} cm^{-1}).[30] Release of adenine base was also indicated by the appearance of a UV-active species on TLC ($CHCl_3/CH_3OH$, 1:1; R_f = 0.72).

LuxS Inhibition Assay. Assay reactions were performed in a buffer containing 50 mM HEPES (pH 7.0), 150 mM NaCl, 150 μM DTNB, and varying concentrations of SRH and inhibitors at room temperature. The reaction was initiated by the addition of LuxS (final concentration of 0.2−0.4 μM) and monitored continuously at 412 nm (ϵ = 14150 M^{-1} cm^{-1}) in a Perkin-Elmer λ25 UV−vis spectrophotometer. The initial rates were calculated from the early regions of the progress curves (~3 min for BsLuxS reactions and ~30 s for VhLuxS and EcLuxS reactions). The remaining activity as a percentage was plotted against each inhibitor concentration to obtain IC_{50} values. The K_I values were calculated from the equations $V/V_0 = (K_M + [S])/\{K_M (1 + [I]/K_I) + [S]\}$ and $K_I = IC_{50}/(1 + [S]/K_M)$, where V and V_0 are the reaction rates in the presence and absence of inhibitors, [S] and [I] are the concentrations of SRH and inhibitor, respectively, and K_M is the Michaelis−Menten constant.

UV−Vis Spectroscopy. Co-BsLuxS was diluted in a buffer containing 50 mM HEPES (pH 7.0), 150 mM NaCl, and varying amounts of inhibitor to a final concentration of 49 μM. UV−vis spectra were recorded 5 min or 1 h after addition of the inhibitors at room temperature. The K_I values were determined by fitting the absorbance increase ΔA at a specific wavelength between 650 and 700 nm against the inhibitor concentration [I] using the equation $\Delta A = \Delta A_{max}[I]/(K_I + [I])$, where ΔA_{max} is the maximal increase in absorbance at saturating concentrations of the inhibitor.

Formation and Isolation of the DPD Derivative. For reactions that involve slow substrates or weakly active LuxS mutants, the DPD formed was converted into its quinoxaline derivative and isolated by HPLC.[16,29,32] Briefly, 1 mM SRH, 5 mg/mL LuxS, and 1 mM 1,2-phenylenediamine were mixed in a pH 7 buffer and incubated for 24 h. Another equivalent of 1,2-phenylenediamine was then added, and the resulting solution was incubated at pH 4−5 for another 24 h followed by ethyl acetate extraction. The crude product was purified by reversed-phase HPLC on a semi-preparative C18 column (Vydac) with a 30 min gradient of 10−100% acetonitrile in water (monitored at 240 nm). The desired compound eluted at ~12 min (~40% acetonitrile).

Crystallization and X-ray Diffraction. Co-BsLuxS was co-crystallized with inhibitors (compounds **10** and **11**) by the hanging drop vapor diffusion method. The well solution consisted of 0.1 M HEPES (pH 7.0) and 2.2 M ammonium sulfate. LuxS protein (10 mg/mL) was mixed with 5.4 mM inhibitor, 25 mM Tris−HCl (pH 8.0), and 100 mM NaCl. The crystals were transferred to a cryoprotectant solution consisting of 0.1 M HEPES (pH 7.0), 2.5 M ammonium sulfate, 15% sucrose, and 5.4 mM inhibitor, mounted in nylon loops, and frozen in liquid nitrogen. X-ray diffraction data were collected at −180 °C using a Rigaku RUH3RHB rotating anode generator and an R-AXIS IV++ image plate detector. The data were processed with CrystalClear software (Molecular Structure Corp.). Crystallographic refinement using CNS[33] began with the structure of the BsLuxS 2-ketone intermediate complex (PDB code 1YCL) after removal of all water molecules, Co^{2+}, and the 2-ketone intermediate. The conjugate gradient minimization and individual temperature factor protocols were used with a maximum likelihood target and overall anisotropic temperature factor and bulk solvent corrections to the data. The inhibitors were added to the model at the later stages of refinement after all of the protein atoms, Co^{2+}, and several water molecules were positioned. Stereochemical parameters for refinement of the inhibitor were generated using the Dundee PRODRG2 server.[34] Model building used the program O,[35] and figures were generated with MOLSCRIPT[36] and RASTER3D.[37]

Acknowledgment. This work was supported by a grant from the National Institutes of Health (AI 062901).

Supporting Information Available: NMR, MS, and HPLC data of target compounds. This material is available free of charge via the Internet at http://pubs.acs.org.

References

(1) Miller, M. B.; Bassler, B. L. Quorum sensing in bacteria. *Annu. Rev. Microbiol.* **2001**, *55*, 165−199.

(2) Bassler, B. L.; Wright, M.; Showalter, R. E.; Silverman, M. R. Intercellular signaling in *Vibrio harveyi*: Sequence and function of genes regulating expression of luminescence. *Mol. Microbiol.* **1993**, *9*, 773−786.

(3) Surette, M. G.; Miller, M. B.; Bassler, B. L. Quorum sensing in *Escherichia coli*, *Salmonella typhimurium*, and *Vibrio harveyi*: A new family of genes responsible for autoinducer production. *Proc. Natl. Acad. Sci. U.S.A.* **1999**, *96*, 1639−1644.

(4) Chen, X.; Schauder, S.; Potier, N.; Van Dorsselaer, A.; Pelczer, I.; Bassler, B. L.; Hughson, F. M. Structural identification of a bacterial quorum-sensing signal containing boron. *Nature* **2002**, *415*, 545−549.

(5) Miller, S. T.; Xavier, K. B.; Campagne, S. R.; Taga, M. E.; Semmelhack, M. F.; Bassler, B. L.; Hughson, F. M. *Salmonella typhimurium* recognizes a chemically distinct form of the bacterial quorum-sensing signal AI-2. *Mol. Cell* **2004**, *15*, 677−687.

(6) Schauder, S.; Shokat, K.; Surette, M. G.; Bassler, B. L. The LuxS family of bacterial autoinducers: Biosynthesis of a novel quorum-sensing signal molecule. *Mol. Microbiol.* **2001**, *41*, 463−476.

(7) Federle, M. J.; Bassler, B. L. Interspecies communication in bacteria. *J. Clin. Invest.* **2003**, *112*, 1291−1299.

(8) Lyon, G. J.; Muir, T. W. Chemical signaling among bacteria and its inhibition. *Chem. Biol.* **2003**, *10*, 1007−1021.

(9) Suga, H.; Smith, K. M. Molecular mechanisms of bacterial quorum sensing as a new drug target. *Curr. Opin. Chem. Biol.* **2003**, *7*, 586−591.

(10) Hentzer, M.; Riedel, K.; Rasmussen, T. B.; Heydorn, A.; Andersen, J. B.; Parsek, M. R.; Rice, S. A.; Eberl, L.; Molin, S.; Høiby, N.; Kjelleberg, S.; Givskov, M. Inhibition of quorum sensing in *Pseudomonas* aeruginosa biofilm bacteria by a halogenated furanone compound. *Microbiology* **2002**, *148*, 87−102.

(11) Ren, D.; Sims, J. J.; Wood, T. K. Inhibition of biofilm formation and swarming of *Bacillus subtilis* by (5Z)-4-bromo-5-(bromomethylene)-3-butyl-2(5H)-furanone. *Lett. Appl. Microbiol.* **2002**, *34*, 293−299.

(12) Hentzer, M.; Wu, H.; Andersen, J. B.; Riedel, K.; Rasmussen, T. B.; Bagge, N.; Kumar, N.; Schembri, M. A.; Song, Z.; Kristoffersen, P.; Manefield, M.; Costerton, J. W.; Molin, S.; Eberl, L.; Steinberg, P.; Kjelleberg, S.; Høiby, N.; Givskov, M. Attenuation of *Pseudomonas aeruginosa* virulence by quorum sensing inhibitors. *EMBO J.* **2003**, *22*, 3803−3815.

(13) Smith, K. M.; Bu, Y.; Suga, H. Induction and Inhibition of *Pseudomonas aeruginosa* quorum sensing by synthetic autoinducer analogs. *Chem. Biol.* **2003**, *10*, 81−89.

(14) Smith, K. M.; Bu, Y.; Suga, H. Library screening for synthetic agonists and antagonists of a *Pseudomonas* aeruginosa autoinducer. *Chem. Biol.* **2003**, *10*, 563−571.

(15) Alfaro, J. F.; Zhang, T.; Wynn, D. P.; Karschner, E. L.; Zhou, Z. S. Synthesis of LuxS inhibitors targeting bacterial cell−cell communication. *Org. Lett.* **2004**, *6*, 3043−3046.

(16) Zhu, J.; Dizin, E.; Hu, X.; Wavreille, A.; Park, J.; Pei, D. *S*-Ribosylhomocysteinase (LuxS) is a mononuclear iron protein. *Biochemistry* **2003**, *42*, 4717−4726.

(17) Lewis, H. A.; Furlong, E. B.; Laubert, B.; Eroshkina, G. A.; batiyenko, Y.; Adams, J. M.; Bergseid, M. G.; Marsh, C. D.; Peat, T. S.; Sanderson, W. E.; Sauder, J. M.; Buchanan, S. G. A structural genomics approach to the study of quorum sensing: Crystal structures of three LuxS orthologs. *Structure* **2001**, *9*, 527−537.

(18) Ruzheinikov, S. N.; Das, S. K.; Sedelnikova, S. E.; Hartley, A.; Foster, S. J.; Horsburgh, M. J.; Cox, A. G.; McCleod, C. W.; Mekhalfia, A.; Blackburn, G. M.; Rice, D. W.; Baker, P. J. The 1.2 Å structure of a novel quorum-sensing protein, *Bacillus subtilis* LuxS. *J. Mol. Biol.* **2001**, *313*, 111−122.

(19) Hilgers, M. T.; Ludwig, M. L. Crystal structure of the quorum-sensing protein LuxS reveals a catalytic metal site. *Proc. Natl. Acad. Sci. U.S.A.* **2001**, *98*, 11169−11174.

(20) Pei, D.; Zhu, J. Mechanism of *S*-ribosylhomocysteinase (LuxS). *Curr. Opin. Chem. Biol.* **2004**, *8*, 492−497.

(21) Rajan, R.; Zhu, J.; Hu, X.; Pei, D.; Bell, C. E. Crystal structure of *S*-ribosylhomocysteinase (LuxS) in complex with a catalytic 2-ketone intermediate. *Biochemistry* **2005**, *44*, 3745−3753.

(22) Marshall, J. A.; Seletsky, B. M.; Luke, G. P. Synthesis of protected carbohydrate derivatives through homologation of threose and erythrose derivatives with chiral γ-alkoxy allylic stannanes. *J. Org. Chem.* **1994**, *59*, 3413−3420.

(23) Hori, H.; Nishida, Y.; Ohrui, H.; Meguro, H. Regioselective de-O-benzylation with Lewis acids. *J. Org. Chem.* **1989**, *54*, 1346−1353.

(24) Congreve, M. S.; Davison, E. C.; Fuhry, M. A. M.; Holmes, A. B.; Payne, A. N.; Robinson, R. A.; Ward, S. E. Selective cleavage of benzyl ethers. *Synlett* **1993**, *9*, 663−664.

(25) Minakawa, N.; Kaga, D.; Kato, Y.; Endo, K.; Tanaka, M.; Sasaki, T.; Matsuda, A. Synthesis and structural elucidation of 1-(3-C-ethynyl-4-thio-β-D-ribofuranosyl)cytosine (4′-thioECyd). *J. Chem. Soc., Perkin Trans. 1* **2002**, 2182−2189.

(26) Ortuño, R. M.; Alonso, D.; Font, J. Enantioselective synthesis of (+)−(S)-β-angelica lactone from L-tartaric acid. *Tetrahedron Lett.* **1986**, *27*, 1079−1080.

(27) Ellman, G. L. Tissue sulfhydryl groups. *Arch. Biochem. Biophys.* **1959**, *82*, 70−77.

(28) Maret, W.; Vallee, B. Cobalt as probe and label of proteins. *Methods Enzymol.* **1993**, *226*, 52−71.

(29) Zhu, J.; Hu, X.; Dizin, E.; Pei, D. Catalytic mechanism of *S*-ribosylhomocysteinase (LuxS): Direct observation of ketone intermediates by ^{13}C NMR spectroscopy. *J. Am. Chem. Soc.* **2003**, *125*, 13379−13381.

(30) Versees, W.; Decanniere, K.; Pelle, R.; Depoorter, J.; Brosens, E.; Parkin, D. W.; Steyaert, J. Structure and function of a novel purine specific nucleoside hydrolase from *Trypanosoma vivax*. *J. Mol. Biol.* **2001**, *307*, 1363−1379.

(31) Salmon, L.; Prost, E.; Merienne, C.; Hardre, R.; Morgant, G. A convenient preparation of aldonohydroxamic acids in water and crystal structure of L-erythronohydroxamic acid. *Carbohydr. Res.* **2001**, *335*, 195−204.

(32) Zhu, J.; Patel, R.; Pei, D. Catalytic mechanism of *S*-ribosylhomocysteinase (LuxS): Stereochemical course and kinetic isotope effect of proton-transfer reactions. *Biochemistry* **2004**, *43*, 10166−10172.

(33) Brünger, A. T.; Adams, P. D.; Clore, G. M.; DeLano, W. L.; Gros, P.; Grosse-Kunstleve, R. W.; Jiang, J. S.; Kuszewski, J.; Nilges, M.; Pannu, N. S.; Read, R. J.; Rice, L. M.; Simonson, T.; Warren, G. L. Crystallography & NMR system: A new software suite for macromolecular structure determination. *Acta Crystallogr., Sect. D* **1998**, *54*, 905−921.

(34) Schuettelkopf, A. W.; Van Aalten, D. M. F. PRODRG: A tool for high-throughput crystallography of protein−ligand complexes. *Acta Crystallogr., Sect. D* **2004**, *60*, 1355−1363.

(35) Jones, T. A.; Zhou, J. Y.; Cowan, S. W.; Kjeldgaard, M. Improved methods for building protein models in electron density maps and the location of errors in these models. *Acta Crystallogr., Sect. A* **1991**, *47*, 110−119.

(36) Kraulis, P. MOLSCRIPT: A program to produce both detailed and schematic plots of protein structures. *J. Appl. Crystallogr.* **1991**, *24*, 946−950.

(37) Merritt, E. A.; Bacon, D. J. Raster3D: Photorealistic molecular graphics. *Methods Enzymol.* **1997**, *277*, 505−524.

JM060047G